Comparative Biochemistry and Physiology, Part B 279 (2025) 111110

Contents lists available at ScienceDirect

Comparative Biochemistry and Physiology, Part B

journal homepage: www.elsevier.com/locate/cbpb

Research Article

Exploring the role of *miR-430* in hybrid fish during embryonic development

Yirui Zhang [1], Chang Wang [1], Jiahao Wu, Ting Liu, Han Wu, Zhonghua Peng, Chengxi Liu, Shengwei Wang, Yan Wang, Kaikun Luo, Jing Wang [*], Shaojun Liu [*]

State Key Laboratory of Developmental Biology of Freshwater Fish, Engineering Research Center of Polyploid Fish Reproduction and Breeding of the State Education Ministry, College of Life Sciences, Hunan Normal University, Changsha 410081, Hunan, PR China

ARTICLE INFO

Editor: Glover Christopher

Keywords:
Hybrid lethality
Maternal-zygotic transition
miR-430
Embryo development

ABSTRACT

miR-430, a microRNA expressed at the maternal-zygotic transition (MZT) stage, plays a vital role in maternal transcript clearance and suppression of primordial germ cell-specific genes. This study investigated the expression and regulation of *miR-430* in goldfish (*Carassius auratus* var., ♀) × rare gudgeon (*Gobiocypris rarus*, ♂) [s-GFRG, survival] and rare gudgeon (♀) × goldfish (♂) [d-RGGF, death] embryos to explore the role of *miR-430* in hybrid fish. Gene sequence comparisons demonstrated that three types of *miR-430* in s-GFRG exhibited similarity to that of the female parent goldfish (GF) and displayed characteristic variation. Conversely, d-RGGF exhibited two *miR-430* variants resembling those of GF and rare gudgeon (RG). In addition, real-time quantitative PCR and whole-mount *in situ* hybridization revealed that the expression trend of *miR-430* was the same in hybrid progenies, and temporal expression was delayed compared to that in the parental embryos. However, *miR-430* expression was significantly lower in d-RGGF than in GF and s-GFRG embryos. Similar to the development of d-RGGF embryos, *miR-430*-silenced s-GFRG embryos exhibited morphological abnormalities including spinal curvature and pericardial cavity enlargement. Overexpression of *miR-430* in d-RGGF embryos effectively rescued somitogenesis and prolonged fry survival. Thus, an abnormal MZT resulting from disturbed *miR-430* expression may contribute to hybrid embryo mortality.

1. Introduction

During early embryonic development, embryos rely entirely on maternally provided materials for developmental processes such as fertilization, cleavage, and the specification of primary cell fates and patterns, due to zygotic transcriptional silencing (Abrams and Mullins, 2009). Following 1–10 cell divisions, embryonic development transitions from maternal factor regulation to zygotic genome activation (ZGA), which defines the maternal-to-zygotic transition (MZT). As a key driver of embryogenesis, the precision and integrity of ZGA is crucial for the normal progression of embryonic development, the orderly differentiation of tissues and organs, and the healthy growth of the individual (Jukam et al., 2017; Vastenhouw et al., 2019). Maternal transcript degradation and ZGA onset, the two central processes of MZT, are strongly interrelated in regulating developmental progression (Zhang et al., 2022). Furthermore, zygotic transcription provides proteins and microRNAs (miRNAs) with a feedback effect that enhances the efficiency of maternal RNA clearance (Walser and Lipshitz, 2011). For example, maternal *nanog* and *pou5f1* activate *miR-430* expression, and *miR-430* is responsible for regulating the zygotic clearance of maternal mRNAs (Lee et al., 2013).

miRNAs are a class of endogenous small non-coding RNAs. By binding to the 3′ untranslated region (UTR) of target genes, miRNAs function as crucial post-transcriptional regulators and often cause the degradation or translation inhibition of target mRNAs (McCreight et al., 2017). Primary miRNAs are first processed by the Drosha-DGCR8 complex into precursor miRNAs (pre-miRNAs), which are then further processed by Dicer into mature miRNAs (Kim et al., 2009). One strand of the mature miRNA is loaded into Argonaute (AGO) proteins, which in turn recruit additional factors to induce mRNA decay(Fabian et al., 2010). Numerous studies have highlighted the essential roles of miRNAs during the MZT across diverse species, including *Drosophila* (Bushati et al., 2008; Örkenby et al., 2023), African clawed frog (*Xenopus laevis*) (Rosa and Brivanlou, 2017; Watanabe et al., 2005), and zebrafish (*Danio rerio*) (Lee et al., 2013). The activation of miRNA transcription at the onset of ZGA represents the only component of a parsimonious switch

* Corresponding authors.
E-mail addresses: hwangjing0826@163.com (J. Wang), lsj@hunnu.edu.cn (S. Liu).
[1] These 2 authors contributed equally to this work.

https://doi.org/10.1016/j.cbpb.2025.111110
Received 22 February 2025; Received in revised form 8 May 2025; Accepted 8 May 2025
Available online 9 May 2025

from the maternal to zygotic transcriptome (Rosa and Brivanlou, 2017).

As one of the earliest zygotic genes expressed during the early development of fish, *miR-430* is known to promote deadenylation and degradation of a large number of maternally expressed mRNAs (Chen et al., 2005; Giraldez et al., 2006; Jiménez-Ruiz et al., 2023). *Nanog* is involved in regulating cellular pluripotency and early embryonic development processes in teleost fish, influencing the proliferation and migration of primordial germ cells (PGCs), and can also be used to evaluate and improve fish egg quality (Yu et al., 2024). DGCR8 and Dicer are essential for miRNA biogenesis (Zhu et al., 2020). As a member of the ribonuclease III family, Dicer plays critical roles in antiviral immunity and microRNA biogenesis while directly mediating the sequence-specific degradation of cognate mRNAs (Lv et al., 2019). AGO proteins associate with small interfering RNAs (siRNAs) or miRNAs to facilitate post-transcriptional gene silencing, primarily *via* mRNA destabilization or translational repression (Tao et al., 2016). In *miR-430*-deficient embryos, these maternal transcripts mentioned above are not adequately degraded and zygotic genes are not fully initiated (Liu et al., 2020b). In addition to the processes of embryogenesis and morphogenesis, *miR-430* plays a crucial role in reproductive development. For example, in many teleost fish, *miR-430* regulates PGCs development by targeting the *C1q-like* factor, *tdrd7*, and *nanos3* in somatic cells (Li et al., 2016; Mei et al., 2014; Sun et al., 2017; Tani et al., 2010). *Tdrd7* performs the function of a regulator of germ plasm localization, which results in the loss of PGC-specific cis-regulatory element accessibility patterns and PGC fate (D'Orazio et al., 2021). In zebrafish, *nanos3* is essential for survival and migration of PGCs (Köprunner et al., 2001). Additionally, *piwil2* is responsible for regulating germ cell differentiation during gametogenesis and gonad development (Houwing et al., 2008; Zhao et al., 2018; Zhou et al., 2012; Zhou and Wang, 2014). As an important maternal TNF/C1q superfamily factor, *C1q-like* factor plays a crucial role in PGC development in *Carassius auratus* (Mei et al., 2014). Furthermore, *miR-430* directly inhibits the expression of *squint* and *lefty* mRNA, thereby ensuring the appropriate dampening and balancing of nodal signaling during mesendoderm induction (Choi et al., 2007). Genetic deletion of *miR-430* results in developmental defects in cell movement, germ layer specification, axis patterning, and organ progenitor formation in zebrafish, contributing to the establishment of an abnormal embryonic body plan (Liu et al., 2020b).

Given its critical role in orchestrating embryonic development, *miR-430* may contribute to the manifestation of hybrid lethality. Hybrid lethality has been observed in many eukaryotes owing to genetic and reproductive regularity barriers (Deng et al., 2019; Liu et al., 2020a; Wang et al., 2019). In our previous study, we obtained several types of surviving hybrid progeny using a series of distant fish crossing experiments (Duan et al., 2007; Liu et al., 2018; Ren et al., 2019). However, many hybrids exhibit abnormal embryonic development and fail to produce viable offspring. Few studies have documented the molecular mechanisms underlying hybrid lethality. Goldfish (*Carassius auratus* var., GF), easily maintained in small laboratory aquaria with year-round periodic spawning and large egg production per event, exhibit embryonic development timing and processes similar to zebrafish. The small-bodied rare gudgeon (*Gobiocypris rarus*, RG) matures quickly, has high reproductive capacity, and spawns year-round. Belonging to distinct genera with significant chromosome number differences, their hybrid embryos serve as convenient experimental models for studying the molecular mechanisms of hybrid lethality. In our previous studies we found that the goldfish (♀) × rare gudgeon (♂) [s-GFRG, survival] hybrids survived, while the embryos of rare gudgeon (♀) × goldfish (♂) [d-RGGF, death] developed abnormally and did not survive (Wang et al., 2025).

In the present study, we investigated miRNA expression and its role in hybrid embryogenesis. Our findings highlighted the potential molecular mechanisms that may underpin hybrid lethality and facilitate a comprehensive understanding of the pivotal role that miRNAs play in fish embryonic development.

2. Materials and methods

2.1. Animals and ethics statement

The specimens (designated as GF and RG) were obtained from the State Key Laboratory of Developmental Biology of Freshwater Fish (Changsha, China). During the breeding season from April to June, sexually mature and healthy individuals were carefully selected as parents and then administered oxytocic agents to induce spawning. A small amount of water was added to a clean glass petri dish. Meanwhile, by gently squeezing the abdomens of female and male fish, fish eggs and sperm were collected into the petri dish. The two were quickly shaken to ensure uniform fertilization. The fertilized eggs were incubated at room temperature. Dead eggs were removed and the water was replaced every three hours. The development of fertilized eggs was observed and documented through stereomicroscopic imaging (MZ16FA; Leica, Wetzlar, Germany). All experimental procedures were approved by the Animal Care Committee of Hunan Normal University and followed the University's guidelines for the care of experimental laboratory animals Welfare (GB/T 35823–2018).

2.2. miR-430 sequencing

Total genomic DNA was extracted with a DNA extraction kit (Sangon, Shanghai, China) and each sample contained 20 embryos. The primers are listed in Table S1. PCR was performed using 1.25 units of Taq DNA polymerase (Takara, Dalian, China), 0.4 μM of each primer, and 2 μL DNA in 25 μL reaction volume. The PCR products were separated and purified by agarose gel electrophoresis and ligated into a pMD18-T vector (Takara, Dalian, China). The vector was subsequently transferred into *Escherichia coli* DH5α. Twenty positive clones were selected for Sanger sequencing. The sequence comparison was conducted by BioEdit 7.2.5 software.

2.3. Real-time quantitative PCR

The staging of embryonic development referred to relevant zebrafish literature and our previously completed work (Kimmel et al., 1995; Wang et al., 2025). Embryos at different stages of development were frozen in liquid nitrogen for total RNA extraction. Total RNA was isolated using TRIzol Reagent (Invitrogen, Carlsbad, CA, USA) and each sample contained 20 embryos. Complementary DNA (cDNA) templates were synthesized from 1 μg total RNA using the miRNA First-Strand Synthesis Kit (Takara, Dalian, China). Real-time quantitative PCR (qPCR) reactions were carried out with 5 μL PowerUp SYBR Green Master Mix (Applied Biosystems, Carlsbad, CA, USA), 0.4 μM of specific forward primers and universal reverse primers, and 5 ng cDNA templates in a final volume of 10 μL in triplicate. The specific forward primer sequence was 5'-TAAGTGCTATTTGTTGGGGTAG-3′. qPCR was performed on a QuantStudio5 instrument (Applied Biosystems, Carlsbad, CA, USA) according to the following protocol: 50 °C for 5 min; 95 °C for 10 min; and 40 cycles of 95 °C for 10 s and 60 °C for 30 s. Melting curve analysis was performed for validation of the amplification specificity.

The stability of housekeeping gene expression was meticulously evaluated using the BestKeeper software. The original Cycle Threshold (Ct) values of the reference genes were inputted in strict compliance with the software instructions (Pfaffl et al., 2004) to derive the standard deviation (SD) and the coefficient of variation (CV) values. The endogenous gene *U6* served as an internal control, and the collected data were analyzed using the Livak ($2^{-\Delta\Delta Ct}$) method and processed with the Statistical Package for the Social Sciences (SPSS), version 27.0. Tests of normality and equality of variance were performed using the Shapiro-Wilk and Levene tests, respectively. Additionally, a one-way analysis of variance (ANOVA) was carried out. At a significance level of 0.05, Tukey's Honestly Significant Difference (HSD) test was employed for the

statistical evaluation of the pairwise differences. The graphs were plotted using GraphPad Prism 7.04 (San Diego, CA, USA).

2.4. Whole-mount in situ hybridization

The *miR-430* transcript fragment was cloned from the cDNA template using PCR primers and then synthesized using T7 RNA polymerase (Thermo Fisher Scientific, Carlsbad, CA, USA) to obtain the desired probe. Following removal of the fertilization membrane using trypsin (Biosharp, Hefei, China), the embryos were fixed overnight in 4 % Paraformaldehyde Fix Solution (PFA) and transferred to 100 % methanol for long term preservation. Whole-mount *in situ* hybridization (WISH) was performed according to standard protocols (Thisse and Thisse, 2008). Five embryos per experimental group were gradient rehydrated and then hybridized with DIG-labeled probe overnight at 70 °C. Anti-digoxigenin-AP Fab fragments (Roche, Basel, Switzerland) in 1 % blocking reagent were used to incubate the embryos overnight at 4 °C. The hybridized probes were detected by incubating the embryos in substrate solution with the NBT and BCIP stock solutions. The embryos were transferred to glycerol and photographed under a stereoscope (MZ16FA; Leica). Staining intensity of embryos was quantified using ImageJ software.

2.5. Microinjection of miRNA mimics and inhibitors

miRNAs specific to *miR-430* mimics, inhibitors, and a negative control (NC) were synthesized by the manufacturer (RiBoBio, Guangzhou, China). One-cell stage embryos of the GF, s-GFRG, and d-RGGF were injected with miRNA-overexpressing mimics [agomirNC (negative control), agomir430] or miRNA-knockdown inhibitors [antagomirNC (negative control), antagomir430] at 10 μM, respectively. One microliter of each miRNA was injected into approximately 100 embryos. Embryos were cultured in clean glass petri dishes containing embryo medium (0.3× Danieau buffer: 17.4 mM NaCl, 0.2 mM KCl, 0.4 mM $MgSO_4$, 0.6 mM $Ca(NO_3)_2$, 10 mM HEPES, pH 7.6) supplemented with 0.01 % (*w/v*) penicillin-streptomycin solution (Beyotime, Shanghai, China) to prevent bacterial contamination at room temperature. The embryos and hatching fish were monitored for two weeks to determine whether they survived or died.

All embryos from each group were frozen in liquid nitrogen immediately and stored at −80 °C. Total RNA was isolated using TRIzol Reagent (Invitrogen, Carlsbad, CA, USA) and each sample contained 20 embryos. The expression levels of *dicer1*, *dgcr8*, *nanog*, *AGOs*, t*drd7*, *nanos3*, *piwil2*, and *C1q-like* factor were measured by qPCR. Total RNA was reverse transcribed to cDNA using HiScript IV All-in-One Ultra RT SuperMix for qPCR (Vazyme, Nanjing, China). The primers are listed in Table S2. *β-actin* was identified in the goldfish genome and used as the negative control for qPCR. The qPCR procedures and data analysis were performed as described in Section 2.3.

3. Results

3.1. Gene sequence alignment analysis

miR-430 has one exon without any introns (Fig. 1A) and is transcribed to mRNA but not translated into protein. To detect genetic variations at the base level in hybrid fish, a single *miR-430* DNA sequence (82 bp) was cloned from parental self-crossing embryos; three types from s-GFRG (GFRG-I, GFRG-II, and GFRG-III), and two types from d-RGGF (RGGF-I and RGGF-II).

Sequence alignment results revealed that the three types of s-GFRG sequences inherited some maternally specific nucleotides and contained base mutations but no paternally specific bases (Fig. 1B). The number of mutant bases was five, eight, and three for GFRG-I, GFRG-II, and GFRG-III, respectively. A total of three paternally specific bases and eight mutant bases were present in RGGF-I, whereas no maternally specific bases were identified. In RGGF-II, there were only four maternally specific bases with no paternally specific or mutant bases (Table 1).

GF and RG sequences of *miR-430* showed high similarity (95.12 %). s-GFRG exhibited high sequence similarity to GF (GFRG-I: 93.90 %; GFRG-II: 90.24 %; GFRG-III: 96.34 %) but low similarity to RG (GFRG-I: 90.24 %; GFRG-II: 86.59 %; GFRG-III: 92.68 %). A comparison of the results obtained revealed a 90.24 % similarity of RGGF-I with GF, whereas the maternal parent demonstrated a similarity of 86.59 %. The *miR-430* sequence in RGGF-II was identical to that in RG (Table 2). Multiple sequence alignment analysis of *miR-430* indicated that all types of s-GFRG showed a tendency toward GF. In contrast, two types of d-RGGF exhibited high similarity to GF and RG.

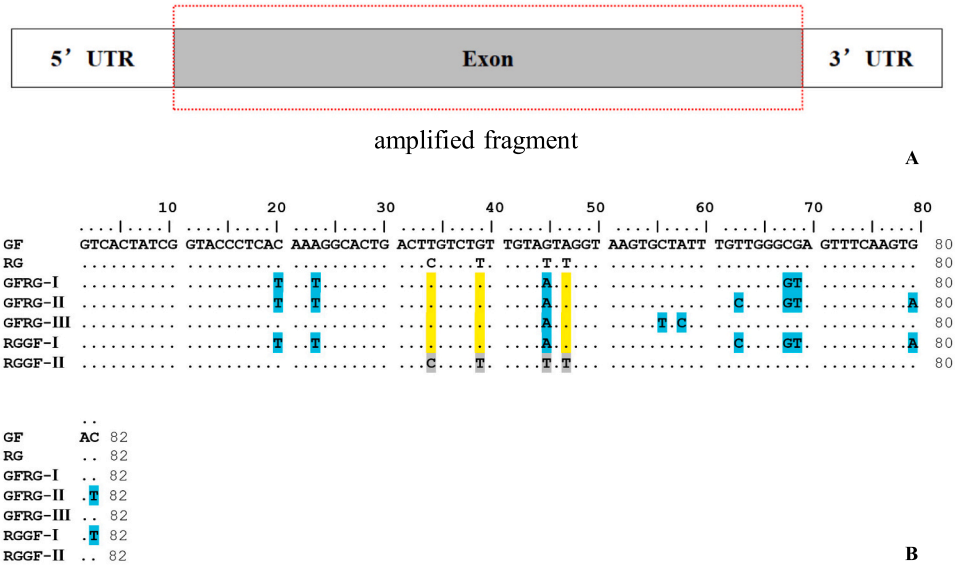

Fig. 1. Genomic structure and sequence alignment of *miR-430*.
A: Genomic structure of *miR-430*. The red box indicates amplified fragment. B: Comparison of *miR-430* DNA sequences. Yellow, gray, and blue rectangles indicate the GF-specific, RG-specific, and mutant bases, respectively. (For interpretation of the references to color in this figure legend, the reader is referred to the web version of this article.)

Table 1
Base changes of *miR-430* DNA fragments in hybrid progeny.

DNA	Sequence length	Total number of differential bases	Number of maternal specific bases	Number of paternal specific bases	Number of mutant bases
GFRG-I	82 bp	8	3	0	5
GFRG-II	82 bp	11	3	0	8
GFRG-III	82 bp	6	3	0	3
RGGF-I	82 bp	11	0	3	8
RGGF-II	82 bp	4	4	0	0

GFRG = goldfish (♀) × rare gudgeon (♂); RGGF = rare gudgeon (♀) × goldfish (♂).

Table 2
Sequence similarity of *miR-430* DNA fragments.

miR-430 DNA	GenBank accession No.	Sequence similarity with GF	Sequence similarity with RG
GF	PQ195648	–	95.12 %
RG	PQ195649	95.12 %	–
GFRG-I	PQ164981	93.90 %	90.24 %
GFRG-II	PQ195650	90.24 %	86.59 %
GFRG-III	PQ195651	96.34 %	92.68 %
RGGF-I	PQ195652	90.24 %	86.59 %
RGGF-II	PQ195653	95.12 %	100 %

GF = goldfish; RG = rare gudgeon.

3.2. Expression patterns of miR-430

To identify the dynamic expression patterns of *miR-430* at different developmental stages in the parental and hybrid offspring, qPCR was conducted. The gene stability analysis conducted with BestKeeper revealed that for the gene *U6*, the SD of the Ct values was 0.82 and the CV was 4.69 in the embryos at different developmental stages of GF (Table S3).

As shown in Fig. 2A, the expression of *miR-430* was activated at the early blastula stage and continued to increase until the late blastula stage in GF embryos. Subsequently, during the early gastrula, late gastrula, and segmentation stages, *miR-430* expression exhibited a dynamic pattern characterized by an initial decline, followed by a peak (the highest expression level), and then a subsequent decrease. *miR-430* expression was initiated at the morula stage in RG embryos; however, the mRNA level of *miR-430* was notably increased until it reached the highest point in the early blastocyst stage and then gradually decreased. The expression was almost undetectable during the early gastrula stage (Fig. 2B).

The expression trends of *miR-430* in the two groups of hybrid offspring were similar; *miR-430* expression was first detected in the early blastula stage and subsequently increased in the late blastula stage. The highest relative expression levels of s-GFRG and d-RGGF were observed in the early gastrula stage, whereas their expression levels were low in the late gastrula stage. Transcription was not detected during the segmentation stage or in fry for both s-GFRG and d-RGGF (Fig. 2C and D).

Notably, *miR-430* exhibited stage-specific differential expression across GF, s-GFRG, and d-RGGF embryos. s-GFRG embryos had significantly higher *miR-430* levels than parental GF at early and late blastula stages, while GF exhibited higher expression than hybrids at the late gastrula stage. In contrast, d-RGGF embryos displayed consistently lower *miR-430* expression than both GF and s-GFRG embryos during the morula, early blastula, late blastula, and late gastrula stages (Fig. 3A-C and E). While the expression of *miR-430* in GF embryos was lower than that in hybrid embryos at the early gastrula stage, s-GFRG embryos maintained significantly higher levels than d-RGGF (Fig. 3D).

3.3. Visualization of the miR-430 transcript

To further investigate the spatial and temporal expression of *miR-430*, WISH was conducted. The intensity of embryo staining reflects the relative abundance of transcripts that hybridize with the probe (Fig. S1). Prior to the morula stage, no difference in the GF embryos was observed between the experimental and control groups. All blastomeres appeared purple at the morula stage and darkened progressively until the late blastula stage. Embryo staining decreased at the onset of the early gastrula stage; however, it rose in the subsequent stage. At the segmentation and fry stages, the embryos remained almost unstained (Fig. 4A and B).

In the RG, from 64 cells to the morula stage, the blastomere exhibited a uniform lilac pigmentation. The cells displayed a dark purple appearance from the early blastula to early gastrula stage. *miR-430* transcripts were almost undetectable during embryonic development after the early gastrula stage (Fig. 4C and D).

In s-GFRG embryos, *miR-430* expression was not detectable until the embryos reached the early blastula stage. The entire blastomere exhibited a purple hue from the early blastula stage until the early gastrula stage. This observation is in stark contrast to that of the control group, which displayed a distinct absence of purple pigmentation throughout the corresponding stage. A decrease in the degree of embryo staining was noted during the late gastrula and segmentation stages. Furthermore, a lilac color was detected in the head cells of the fry, indicating that *miR-430* was expressed in the brain (Fig. 5A and B).

Consistent with the qPCR results, *miR-430* expression was not present until the early blastula stage in d-RGGF embryos. From the late blastula stage to early gastrula stage, all blastoderm cells were stained purple. The level of embryo staining was extremely low at the late gastrula stage. Embryos at the segmentation and fry stages were almost unstained (Fig. 5C and D).

3.4. Defective forms of miR-430

To investigate how *miR-430* affects embryonic development, the consequences of *miR-430* knock down and overexpression were examined. Three different concentrations of agomir430 and antagomir430 were injected into single-cell stage embryos of the parental goldfish (Fig. 6A). No morphological abnormalities or changes in mortality were observed in the 2 μM and 5 μM treatment groups. Similar to d-RGGF, embryos treated with 10 μM antagomir430 showed morphological abnormalities (spinal curvature and enlarged pericardial cavity) and higher mortality compared to that of the other treatment groups (Fig. 6B and C).

Changes in target gene expression after *miR-430* knockdown and overexpression were measured using qPCR. The experimental results of the stability analysis performed by Bestkeeper indicated that for *β-actin*, the SD of the Ct values was 0.79 and the CV was 3.42 across different treatment groups of GF (Table S1). All maternally provided transcripts and primordial specific genes affected by *miR-430* were negatively correlated with *miR-430* expression levels. Notably, insignificant changes were observed following 2 μM injection treatment. The expression levels of *dicer1*, *ago1*, *ago4*, *tdrd7*, *nanos3*, and *piwil2* were increased but not significantly under 5 μM *miR-430*-inhibition treatment (Fig. 6D, G, and I-L). When the concentrations were increased to 10 μM, compared to the control group, all the *miR-430* target genes showed significant changes in their expression levels. Based on these results, 10 μM agomir430, antagomir430, and their relevant negative controls were injected into single-cell stage embryos of s-GFRG and d-RGGF, respectively.

A comparison of the negative control treatment with the blank control group revealed that the former did not significantly affect the embryonic morphology or mortality. We analyzed the effects of *miR-430* deletion on phenotype. All resultant embryos developed normally

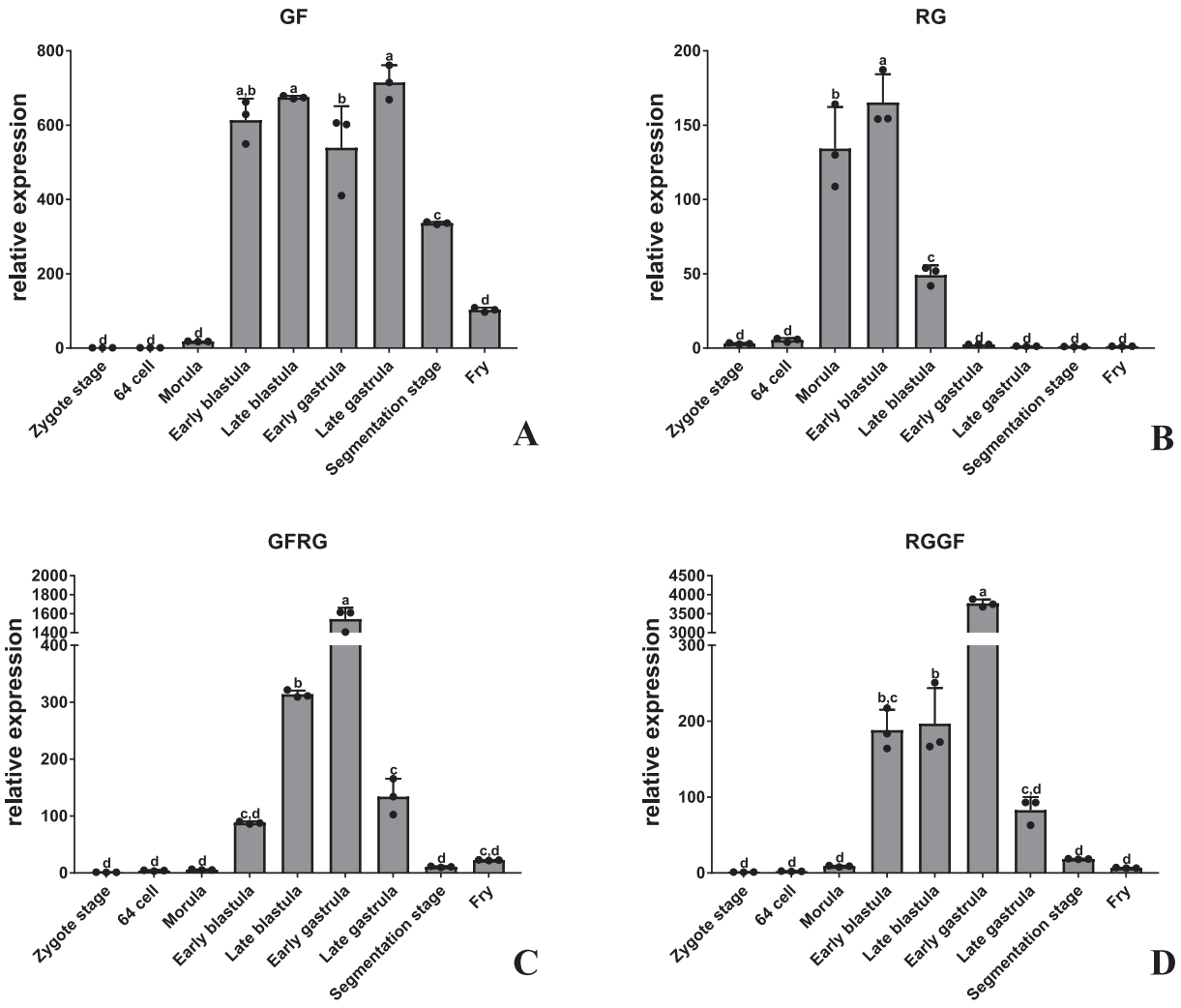

Fig. 2. Expression patterns of *miR-430* in embryos.
A: Histograms of *miR-430* expression in GF embryos; B: Histograms of *miR-430* expression in RG embryos; C: Histograms of *miR-430* expression in s-GFRG embryos; D: Histograms of *miR-430* expression in d-RGGF embryos. Relative expression levels are presented as the mean ± standard deviation of three replicates. Different letters on the graph indicate significant differences($P < 0.05$).

during the cleavage and blastula stages. However, many malformations and high mortality rates were observed in *miR-430*-silenced s-GFRG and d-RGGF embryos during segmentation. In *miR-430*-silenced embryos, the anterior-posterior body axis exhibited a reduction in extension, while the spine demonstrated a substantial degree of curvature (Fig. 7A-D). Moreover, *miR-430* downregulation in embryos disrupted brain regionalization and enlarged the pericardial cavity at 48 h post-fertilization (hpf). Compared to the high survival rate in the control group, most *miR-430*-silenced s-GFRG embryos died within 8 d. Few deformed fry hatched, and all died within 3 d of hatching in the d-RGGF control group (Fig. 7G). Notably, the exogenous re-expression of *miR-430* effectively reduced the malformation rate and prolonged the life-span of fry up to 12 d after hatching (Fig. 7E and F).

miR-430 knockdown and overexpression were also confirmed using qPCR. In embryos from different treatment groups of GFRG and RGGF at the early gastrula stage, the SD of the Ct values of *β-actin* was 0.93 and the CV was 4.36. Moreover, in embryos from different treatment groups of GFRG and RGGF at the late gastrula stage, the SD of the Ct values of *β-actin* was 0.47 and the CV was 2.5(Table S1). The significant differential expression of *miR-430* was confirmed in the s-GFRG and d-RGGF control groups (Fig. 7H). Additionally, at the early gastrula stage, there was no significant difference in the expression levels of *dicer1*, *ago1*, and *ago4* between the four groups, whereas impaired clearance of *dgcr8*, *nanog*, and *ago2* was found in d-RGGF compared to s-GFRG (Fig. 8A-F). As shown in Fig. 8G-J, no significant variations were detected in the expression levels of *tdrd7*, *nanos3*, and *piwil2* among the four groups, whereas the level of *C1q-like* factor was higher in s-GFRG than in d-RGGF at the early gastrula stage. The effects of *miR-430* expression were observed at the late gastrula stage in s-GFRG and d-RGGF. *miR-430* overexpression in d-RGGF cells significantly reduced the *dicer1*, *dgcr8*, *nanog*, *ago2* and *ago4* transcript levels. The clearance of maternal *ago2* and *ago4* in s-GFRG was significantly higher than that in d-RGGF. Furthermore, mRNA expression levels of *dicer1*, *dgcr8*, *nanog*, *ago1*, and *ago2* were upregulated following *miR-430* silencing, indicating that the embryos had lost the inhibitory effect of *miR-430*. Upregulation of *miR-430* reduced the expression levels of *dicer1*, *dgcr8*, *nanog*, *ago1*, *ago2*, and *ago4*, with remarkable differences between *nanog*, *ago2*, and *ago4* (Fig. 8K-P). The transcriptional levels of *tdrd7*, *nanos3*, *piwil2*, and *C1q-like* factor were substantially increased in response to the knockdown of *miR-430* in s-GFRG embryos. Consistent with this, the overexpression of *miR-430* significantly decreased the expression of zygotically expressed transcripts (Fig. 8Q-T).

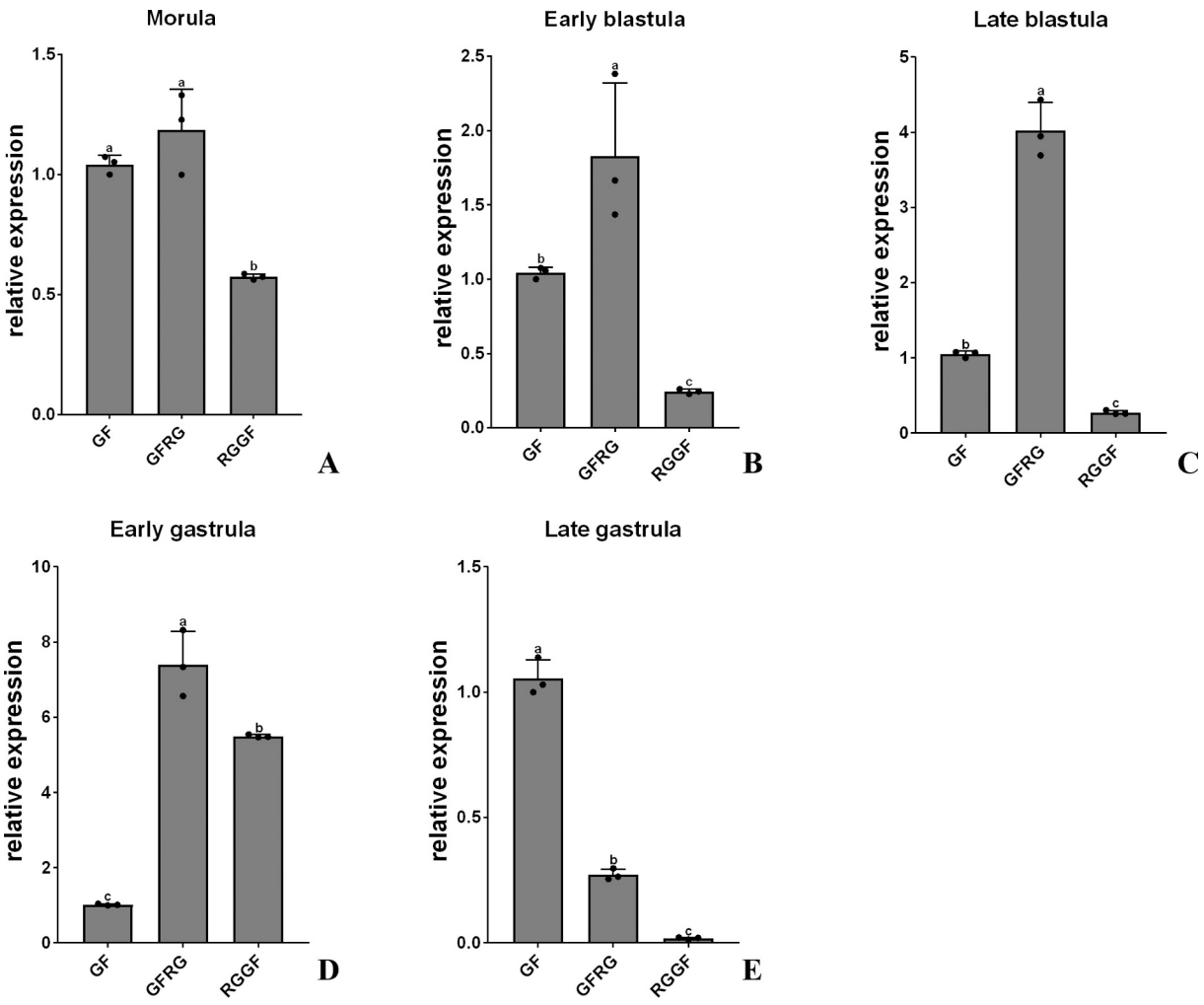

Fig. 3. Histograms of *miR-430* expression in GF and hybrid embryos.
Relative expression levels are presented as the mean ± standard deviation of three replicates. Different letters on the graph indicate significant differences($P < 0.05$).

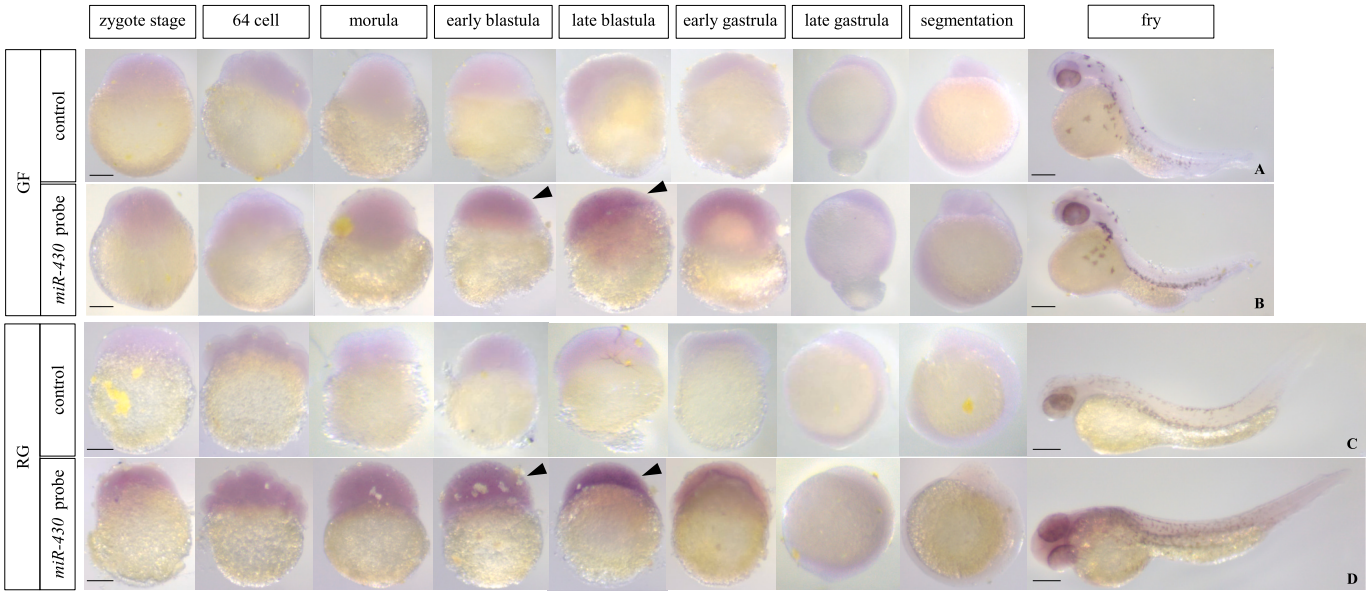

Fig. 4. Visualization of the *miR-430* transcript in parental embryos.
A: Control group of GF embryos; B: Experimental group of GF embryos; C: Control group of RG embryos; D: Experimental group of RG embryos. Images show representative individuals from five replicates. The black arrow indicates the *miR-430* expression position. Scale bar = 0.5 mm.

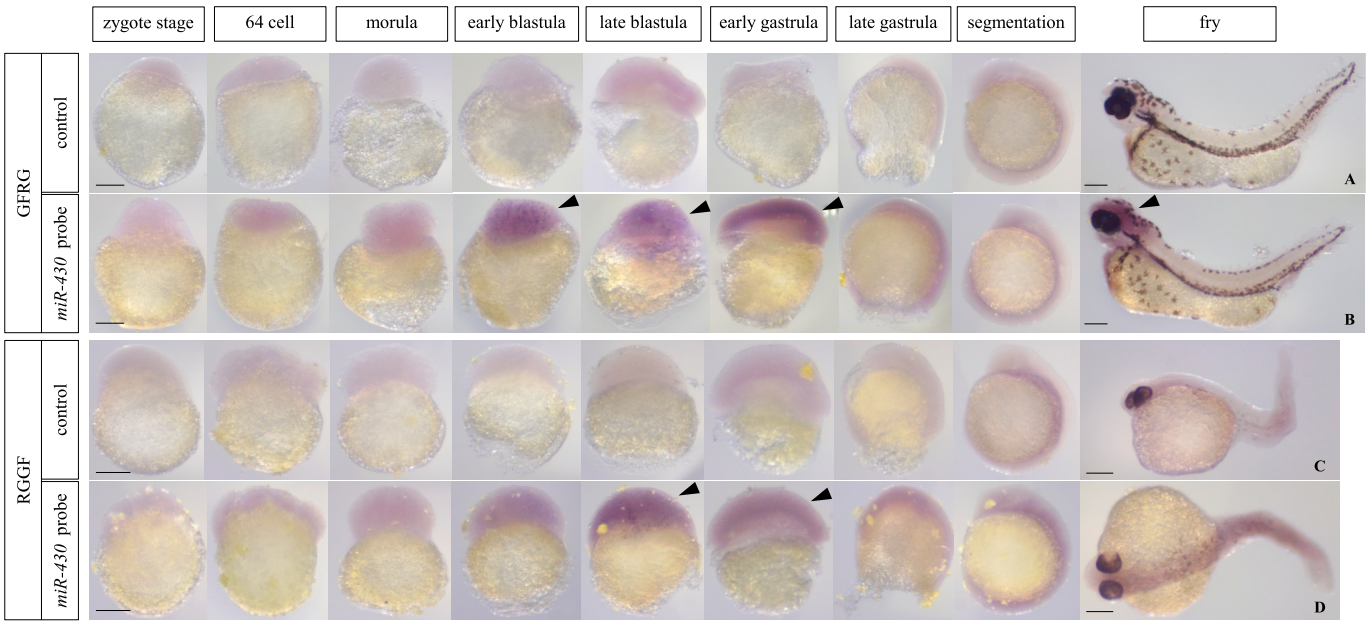

Fig. 5. Visualization of the *miR-430* transcript in hybrid embryos.
A: Control group of s-GFRG embryos; B: Experimental group of s-GFRG embryos; C: Control group of d-RGGF embryos; D: Experimental group of d-RGGF embryos. Images show representative individuals from five replicates. The black arrow indicates the *miR-430* expression position. Scale bar = 0.5 mm.

4. Discussion

4.1. Types of miR-430

Despite the relatively simple structure and short length of *miR-430*, different base sites were revealed and these may be associated with species specificity. In d-RGGF, the two *miR-430* genotypes resembled the maternal and paternal genotypes. The three *miR-430* genotypes in s-GFRG were similar to those in GF, and several mutation sites were identified.

Two divergent genomes that evolve independently in parents are reunited into a common nucleus at the time of hybrid offspring formation, resulting in hybrid incompatibilities that diminish hybrid viability or fertility (Moran et al., 2021). Nevertheless, heterologous recombination and base mutations have been commonly observed in hybrid fish, which are considered important genetic traits that decrease genome incompatibility between different species (Wang et al., 2015). Previous studies in our laboratory indicated that s-GFRG is allotriploid whereas d-RGGF is diploid. An increased genome size can produce a higher probability of heterologous recombination, which can also be accompanied by better viability and adaptability (Comai, 2005). In contrast, simple genome fusion between the parents of two different species causes incompatibility of the genetic material in d-RGGF. It is evident that extensive recombinations and mutations have the capacity to reduce genome incompatibility, thus resulting in a complete alteration of the developmental fates of s-GFRG and d-RGGF (Wang et al., 2025).

4.2. Expression of miR-430

The expression stability of the reference genes utilized in this investigation was meticulously appraised using the BestKeeper software. Genes exhibiting a SD of Ct values below 1, coupled with a minimal CV, were deemed to demonstrate consistent expression across diverse experimental samples (Lai et al., 2024). Consequently, the reference genes adopted in this study were validated as suitable for use.

Our findings showed that the transcription of *miR-430* began in the early blastula stage in GF compared to the earlier morula stage in RG. This coincides with the MZT stage, which occurs according to species-specific timing. Moreover, the presence of *miR-430* transcripts was detected in all blastoderm cells from the morula through to the early gastrula stage of development, suggesting ubiquitous expression in the early embryo. *miR-430* expression is robust during axis formation, but it exhibits a decline in the somite form. The temporal expression of *miR-430* is broadly consistent with that reported in zebrafish and medaka (*Oryzias latipes*) (Giraldez et al., 2006; Tani et al., 2010), suggesting evolutionary conservation of its regulatory and functional roles. This consistency reflects the miRNA's involvement in fundamental biological processes essential for teleost survival, thereby minimizing evolutionary divergence in its expression dynamics and molecular functions.

Compared to the parents, the emergence of the MZT was delayed in the hybrid progeny, indicating potential disruptions in early embryonic development programs. No discrepancies were detected in the temporal and spatial expression patterns of *miR-430* between s-GFRG and d-RGGF embryos; however, a substantial discrepancy was observed in the expression levels. Specifically, *miR-430* expression levels in GF and s-GFRG embryos were significantly higher than those in d-RGGF embryos, which likely results from genomic instability associated with hybridization.

As previously reported, disparities in chromosome number between parental entities result in alterations in the chromosome number of distant hybrids (Liu, 2010). This genomic instability, arising from the combination of heterologous genomes directly results in changes in hybrid progeny gene transcription, such as gene silencing, upregulation or downregulation of expression, non-functionalization, sub-functionalization, and neofunctionalization (Adams and Wendel, 2005; Song et al., 2012). These transcriptional disruptions commonly disrupt normal embryonic development, ultimately culminating in embryotoxicity or lethality (Chen et al., 2018; Zhang et al., 2014),which aligns with the widely accepted hypothesis that gene expression variation plays important roles in speciation and adaptive evolution (Romero et al., 2012).

The elevated ploidy in s-GFRG likely activated a dosage compensation mechanism, as evidenced by the significantly higher *miR-430* expression compared to d-RGGF. In lower vertebrates, dosage compensation is essential for maintaining genomic stability and ensuring the evolutionary success of polyploid lineages (Pala et al., 2008). Furthermore, the upregulation of growth-related genes in triploids results in an accelerated growth rate compared with that of diploids (Ren et al.,

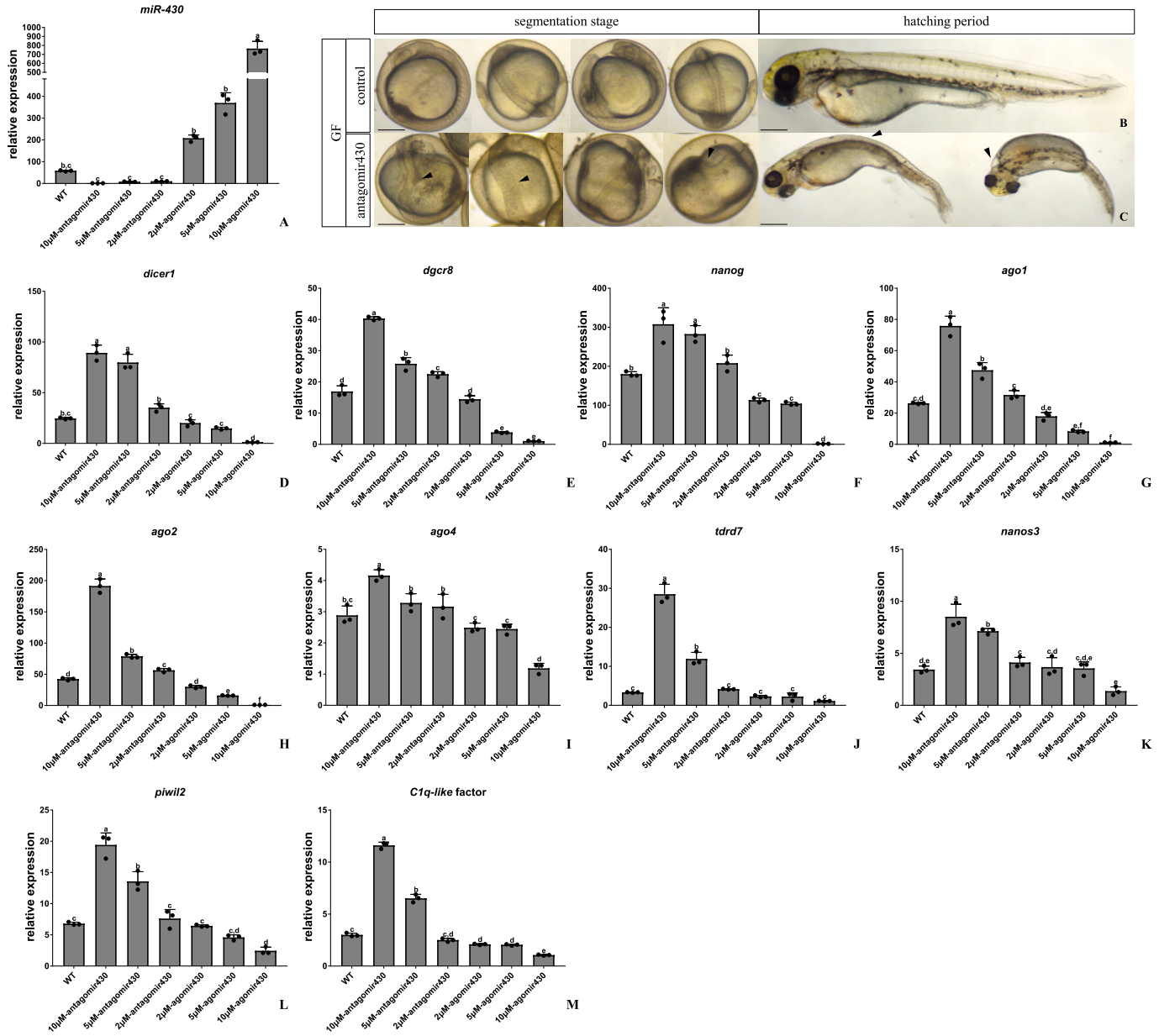

Fig. 6. Molecular and phenotypic consequences of *miR-430* deletion in GF embryos.
A: qPCR results of *miR-430* in GF embryos after injection of agomir430 and antagomir430; B: GF embryos as a control; C: Morphogenesis of GF embryos injected with 10 μM antagomir430; D-I: Relative expression of *dicer1*, *dgcr8*, *nanog*, and *AGOs* in GF embryos; J-M: Relative expression of *tdrd7*, *nanos3*, *piwil2*, and *C1q-like* factor in GF embryos. Embryos were collected during the late blastula stage. WT = wild type. Relative expression levels are presented as the mean ± standard deviation of three replicates. Different letters on the graph indicate significant differences($P < 0.05$). Scale bar = 0.5 mm.

2017). In contrast, genomic instability resulting from distant hybridization led to reduced *miR-430* levels in d-RGGF embryos. Subsequently, these transcriptional regulatory disruptions likely perturbed the *miR-430*-governed regulatory networks, resulting in abnormal gene functionality. Ultimately, such molecular dysregulation may represent a key contributing factor to the observed embryonic developmental abnormalities and lethality in d-RGGF.

4.3. Function of miR-430

Different phenotypes can be attributed to the dysregulation of specific genes and target mRNAs. Knockdown of *miR-430* led to severe axial defects in s-GFRG, with most embryos showing short and curved body axes and an enlarged pericardial cavity. These defects are consistent with those observed in wild-type d-RGGF embryos. In contrast, overexpression of *miR-430* in d-RGGF embryos rescued abnormal embryo phenotypes and prolonged fry survival.

miR-430 is widely expressed and functional in all cells. The knockdown of *miR-430* restricted to the organizer and Kupffer's vesicle progenitor cells recapitulates looping defects observed in whole-embryo knockdown, suggesting that *miR-430* is a key regulatory factor influencing the development of the left/right asymmetry in gut and heart (Brown et al., 2022). *Dicer* is essential for miRNA biogenesis, and reintroduction of *miR-430* can rescue morphogenetic defects during gastrulation and brain ventricle development in *dicer*-deficient zebrafish embryos (Giraldez et al., 2005). It has been proposed that *miR-430* coordinates the cell divisions that induce neural tube morphogenesis (Takacs and Giraldez, 2016). Phenotypically, the signal of the *miR-430* probe appears in the brain ventricular system of s-GFRG fry, suggesting that *miR-430* may be involved in brain ventricle formation and

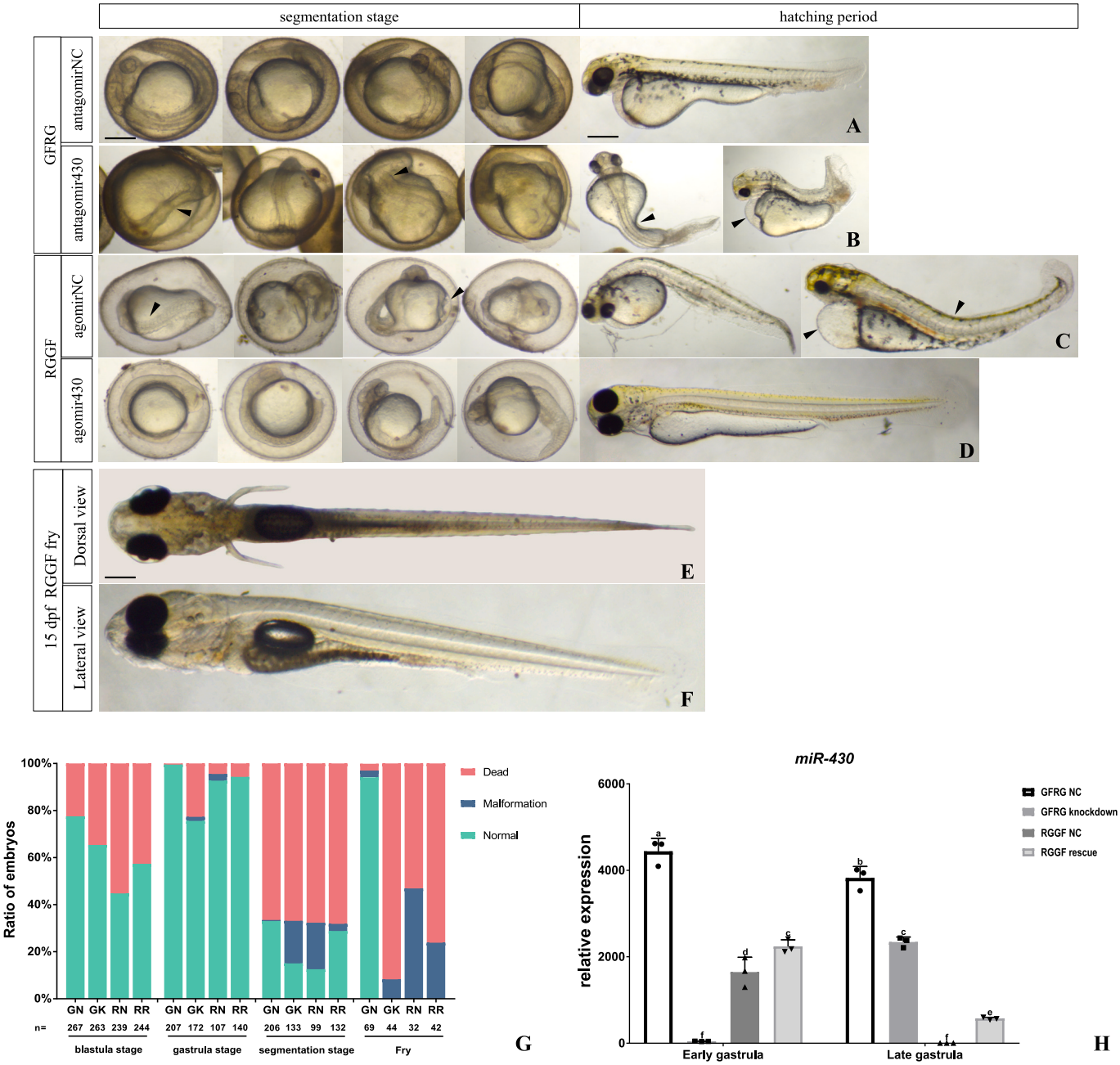

Fig. 7. Phenotypic consequences of *miR-430* deletion and overexpression.
A-D: Morphogenesis of s-GFRG and d-RGGF embryos after injection; *E*-F: Morphogenesis in d-RGGF fry injected with agomir430 (15 dpf); E: Dorsal view; F: Lateral (left side) view. Scale bar = 0.5 mm. G: Ratio of embryos in different classes. GN = GFRG NC; GK = GFRG Knockdown; RN = RGGF NC; RR = RGGF Rescue. H: qPCR results for *miR-430* in hybrid embryos after injection. Relative expression levels are presented as the mean ± standard deviation of three replicates. Different letters on the graph indicate significant differences($P < 0.05$).

subsequent morphogenesis.

Clearance of maternal mRNAs is required for MZT and promotes the establishment of global heterochromatin (Laue et al., 2019). The biogenesis and function of *miR-430* depends on maternally provided transcripts, which in turn facilitate the degradation of these maternally provided transcripts (Lee et al., 2013; Liu et al., 2020b). Inhibition of *miR-430* translation occurred at 4 hpf, while significant mRNA decay was detected only at 6 hpf (Bazzini et al., 2012). The functional relevance of maternal transcript clearance by *miR-430* was confirmed by showing that decreased *miR-430* levels were correlated with the accumulation of *nanog*, *dicer1*, *dgcr8*, and *AGOs* (Fischer et al., 2019). Failure in *nanog* degradation due to *miR-430* deficiency may lead to abnormal organization of yolk microtubules required for ectoderm development and incorrect formation of actin structures in the yolk syncytial layer (YSL), ultimately resulting in severe disruptions to the ectodermal axis and massive cell death at the terminal stage of embryonic development (Veil et al., 2018). These results suggest that *miR-430* facilitates the transition from a maternal to zygotic state (Liu et al., 2020b). The prolonged presence of maternally supplied transcripts may be a barrier to full ZGA.

In this study, qPCR confirmed that the deletion of *miR-430* causes an increase in *tdrd7*, *nanos3*, *piwil2*, and *C1q-like* factor expression in s-GFRG embryos, consistent with the established ability of agomir430 to reduce the expression levels of primordial-specific genes. These data

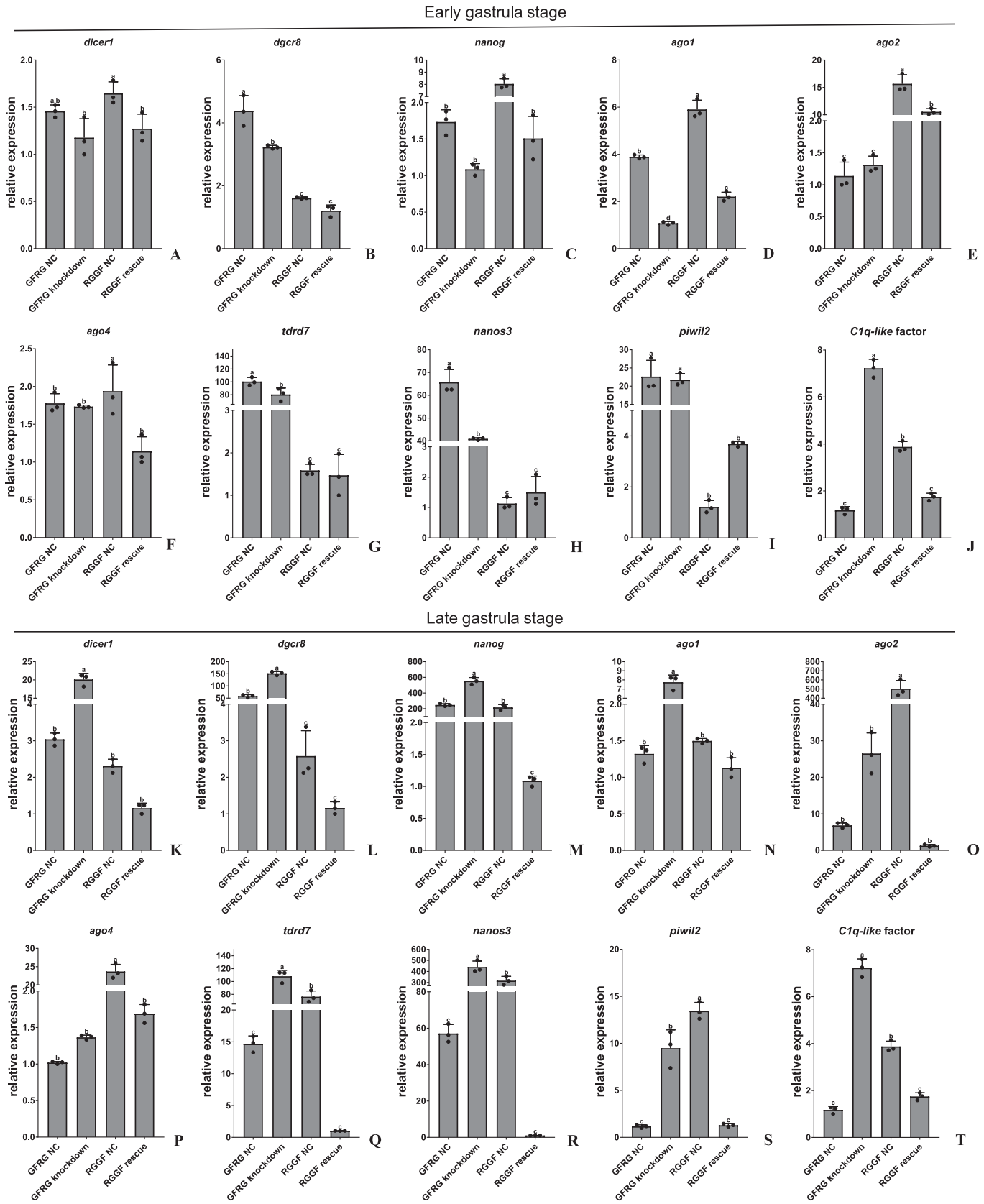

Fig. 8. Real-time quantitative PCR results of target genes of *miR-430* in different treatment groups.
A-J: Relative expression of *dicer1*, *dgcr8*, *nanog*, *AGOs*, *tdrd7*, *nanos3*, *piwil2*, and *C1q-like* factor in early gastrula stage in hybrid embryos; K-T: Relative expression of *dicer1*, *dgcr8*, *nanog*, *AGOs*, *tdrd7*, *nanos3*, *piwil2*, and *C1q-like* factor in late gastrula stage in hybrid embryos. Relative expression levels are presented as the mean ± standard deviation of three replicates. Different letters on the graph indicate significant differences($P < 0.05$).

suggest that *miR-430* plays an essential role in controlling the survival, proliferation, and migration of fish PGCs during development (Tani et al., 2010). Further research is now needed to clarify whether the redundancy of primordial-specific genes leads to changes in the somatic differentiation and divergent fate of the embryonic germline and later development in hybrid fish.

5. Conclusion

In summary, our study reveals that genetic material coordination between the two distantly related parental genomes in s-GFRG embryos is higher than in d-RGGF embryos, likely due to genetic recombination and mutational events. *MiR-430* functions in maternal transcript degradation and PGCs development, and its expression levels are significantly higher in s-GFRG than in d-RGGF embryos. Disturbed expression of *miR-430* in d-RGGF causes the accumulation of maternal transcripts, and the zygotic genome is not fully activated. As a result, the d-RGGF embryos develop abnormally and eventually die. Therefore, a normal MZT is an important factor for the survival of distant hybrid offspring. By comparing *miR-430* genetic variations, spatiotemporal expression patterns, and functional roles during embryonic development between parental and distant hybrid offspring, this study investigates the impact of zygotic gene activation and function on fish hybrid embryo development. These findings provide new insights into hybrid lethality and may also benefit fish crossbreeding.

CRediT authorship contribution statement

Yirui Zhang: Writing – original draft, Investigation, Data curation, Conceptualization. **Chang Wang:** Resources, Investigation, Data curation. **Jiahao Wu:** Resources, Investigation, Data curation. **Ting Liu:** Investigation, Data curation. **Han Wu:** Investigation, Formal analysis, Data curation. **Zhonghua Peng:** Writing – review & editing. **Chengxi Liu:** Writing – review & editing. **Shengwei Wang:** Writing – review & editing. **Yan Wang:** Writing – review & editing. **Kaikun Luo:** Writing – review & editing. **Jing Wang:** Writing – review & editing, Project administration, Funding acquisition, Conceptualization. **Shaojun Liu:** Writing – review & editing, Supervision, Funding acquisition, Conceptualization.

Funding

This work was supported by the National Key Research and Development Program of China (2023YFD2400202), the National Natural Science Foundation of China (Grants No. 32373117, 32293251, and U19A2040), the Special Funds for Construction of Innovative Provinces in Hunan (Grant No. 2021NK1010), the Earmarked Fund for Agriculture Research System of China (Grant No. CARS-45), the Laboratory of Lingnan Modern Agriculture Project (Grant No. NT2021008), the 111 Project (D20007), and Special Science Found of Nansha-South China Agricultural University Fishery Research Institute, Guangzhou.

Declaration of competing interest

The authors declare that they have no conflict of interest.

Acknowledgments

We thank editage (www.editage.cn) for linguistic assistance and Hunan Yuelu Mountain Scienece and Technology Co.Ltd. for Aquatic Breeding.

Appendix A. Supplementary data

Supplementary data to this article can be found online at https://doi.org/10.1016/j.cbpb.2025.111110.

Data availability

Data will be made available on request.

References

Abrams, E.W., Mullins, M.C., 2009. Early zebrafish development: it's in the maternal genes. Curr. Opin. Genet. Dev. 19, 396–403. https://doi.org/10.1016/j.gde.2009.06.002.

Adams, K.L., Wendel, J.F., 2005. Novel patterns of gene expression in polyploid plants. Trends Genet. 21, 539–543. https://doi.org/10.1016/j.tig.2005.07.009.

Bazzini, A.A., Lee, M.T., Giraldez, A.J., 2012. Ribosome profiling shows that *miR-430* reduces translation before causing mRNA decay in zebrafish. Science 336, 233–237. https://doi.org/10.1126/science.1215704.

Brown, W., Bardhan, A., Darrah, K., Tsang, M., Deiters, A., 2022. Optical control of microRNA function in zebrafish embryos. J. Am. Chem. Soc. 144, 16819–16826. https://doi.org/10.1021/jacs.2c04479.

Bushati, N., Stark, A., Brennecke, J., Cohen, S.M., 2008. Temporal reciprocity of miRNAs and their targets during the maternal-to-zygotic transition in *Drosophila*. Curr. Biol. 18, 501–506. https://doi.org/10.1016/j.cub.2008.02.081.

Chen, P.Y., Manninga, H., Slanchev, K., Chien, M.C., Russo, J.J., Ju, J.Y., Sheridan, R., John, B., Marks, D.S., Gaidatzis, D., Sander, C., Zavolan, M., Tuschl, T., 2005. The developmental miRNA profiles of zebrafish as determined by small RNA cloning. Genes Dev. 19, 1288–1293. https://doi.org/10.1101/gad.1310605.

Chen, J., Luo, M., Li, S.N., Tao, M., Ye, X.L., Duan, W., Zhang, C., Qin, Q.B., Xiao, J., Liu, S.J., 2018. A comparative study of distant hybridization in plants and animals. Sci. China Life Sci. 61, 285–309. https://doi.org/10.1007/s11427-017-9094-2.

Choi, W.Y., Giraldez, A.J., Schier, A.F., 2007. Target protectors reveal dampening and balancing of nodal agonist and antagonist by *miR-430*. Science 318, 271–274. https://doi.org/10.1126/science.1147535.

Comai, L., 2005. The advantages and disadvantages of being polyploid. Nat. Rev. Genet. 6, 836–846. https://doi.org/10.1038/nrg1711.

Deng, J.Q., Fang, L., Zhu, X.F., Zhou, B.L., Zhang, T.Z., 2019. A *CC-NBS-LRR* gene induces hybrid lethality in cotton. J. Exp. Bot. 70, 5145–5156. https://doi.org/10.1093/jxb/erz312.

D'Orazio, F.M., Balwierz, P.J., González, A.J., Guo, Y.X., Hernández-Rodríguez, B., Wheatley, L., Jasiulewicz, A., Hadzhiev, Y., Vaquerizas, J.M., Cairns, B., Lenhard, B., Müller, F., 2021. Germ cell differentiation requires Tdrd7-dependent chromatin and transcriptome reprogramming marked by germ plasm relocalization. Dev. Cell 56, 641. https://doi.org/10.1016/j.devcel.2021.02.007.

Duan, W., Qin, Q.B., Chen, S., Liu, S.J., Wang, J., Zhang, C., Sun, Y.D., Liu, Y., 2007. The formation of improved tetraploid population of red crucian carp x common carp hybrids by androgenesis. Sci China Ser C. 50, 753–761. https://doi.org/10.1007/s11427-007-0090-5.

Fabian, M.R., Sonenberg, N., Filipowicz, W., 2010. Regulation of mRNA translation and stability by microRNAs. Annu. Rev. Biochem. 79, 351–379. https://doi.org/10.1146/annurev-biochem-060308-103103.

Fischer, P., Chen, H., Pacho, F., Rieder, D., Kimmel, R.A., Meyer, D., 2019. FoxH1 represses *miR-430* during early embryonic development of zebrafish via non-canonical regulation. BMC Biol. 17. https://doi.org/10.1186/s12915-019-0683-z.

Giraldez, A.J., Cinalli, R.M., Glasner, M.E., Enright, A.J., Thomson, J.M., Baskerville, S., Hammond, S.M., Bartel, D.P., Schier, A.F., 2005. MicroRNAs regulate brain morphogenesis in zebrafish. Science 308, 833–838. https://doi.org/10.1126/science.1109020.

Giraldez, A.J., Mishima, Y., Rihel, J., Grocock, R.J., Van Dongen, S., Inoue, K., Enright, A.J., Schier, A.F., 2006. Zebrafish *miR-430* promotes deadenylation and clearance of maternal mRNAs. Science 312, 75–79. https://doi.org/10.1126/science.1122689.

Houwing, S., Berezikov, E., Ketting, R.F., 2008. Zili is required for germ cell differentiation and meiosis in zebrafish. EMBO J. 27, 2702–2711. https://doi.org/10.1038/emboj.2008.204.

Jiménez-Ruiz, C.A., de la Herrán, R., Robles, F., Navajas-Pérez, R., Cross, I., Rebordinos, L., Ruiz-Rejón, C., 2023. *miR-430* microRNA family in fishes: molecular characterization and evolution. Animal 13. https://doi.org/10.3390/ani13152399.

Jukam, D., Shariati, S.A.M., Skotheim, J.M., 2017. Zygotic genome activation in vertebrates. Dev. Cell 42, 316–332. https://doi.org/10.1016/j.devcel.2017.07.026.

Kim, V.N., Han, J., Siomi, M.C., 2009. Biogenesis of small RNAs in animals. Nat. Rev. Mol. Cell Biol. 10, 126–139. https://doi.org/10.1038/nrm2632.

Kimmel, C.B., Ballard, W.W., Kimmel, S.R., Ullmann, B., Schilling, T.F., 1995. Stages of embryonic development of the zebrafish. Developmental Dynamics 203, 253–310. https://doi.org/10.1002/aja.1002030302.

Köprunner, M., Thisse, C., Thisse, B., Raz, E., 2001. A zebrafish nanos-related gene is essential for the development of primordial germ cells. Gene Dev. 15, 2877–2885. https://doi.org/10.1101/gad.212401.

Lai, T.H., Hwang, J.S., Ngo, Q.N., Lee, D.K., Kim, H.J., Kim, D.R., 2024. A comparative assessment of reference genes in mouse brown adipocyte differentiation and thermogenesis in vitro. Adipocyte 13, 2330355. https://doi.org/10.1080/21623945.2024.2330355.

Laue, K., Rajshekar, S., Courtney, A.J., Lewis, Z.A., Goll, M.G., 2019. The maternal to zygotic transition regulates genome-wide heterochromatin establishment in the zebrafish embryo. Nat. Commun. 10, 1551. https://doi.org/10.1038/s41467-019-09582-3.

Lee, M.T., Bonneau, A.R., Takacs, C.M., Bazzini, A.A., DiVito, K.R., Fleming, E.S., Giraldez, A.J., 2013. Nanog, Pou5f1 and SoxB1 activate zygotic gene expression

during the maternal-to-zygotic transition. Nature 503, 360–364. https://doi.org/10.1038/nature12632.
Li, M.J., Tan, X.G., Sui, Y.L., Jiao, S., Wu, Z.H., You, F., 2016. Conserved elements in the 3'UTR of olive flounder are responsible for the selective retention of RNA in germ cells. Comp Biochem Phys B. 198, 66–72. https://doi.org/10.1016/j.cbpb.2016.04.002.
Liu, S.J., 2010. Distant hybridization leads to different ploidy fishes. Sci. China Life Sci. 53, 416–425. https://doi.org/10.1007/s11427-010-0057-9.
Liu, Q.F., Qi, Y.H., Liang, Q.L., Xu, X.J., Hu, F.Z., Wang, J., Xiao, J., Wang, S., Li, W.H., Tao, M., Qin, Q.B., Zhao, R.R., Yao, Z.Z., Liu, S.J., 2018. The chimeric genes in the hybrid lineage of *Carassius auratus cuvieri* (♀)×*Carassius auratus red var.* (♂). Sci. China Life Sci. 61, 1079–1089. https://doi.org/10.1007/s11427-017-9306-7.
Liu, Q.F., Liu, J.M., Yuan, L.J., Li, L., Tao, M., Zhang, C., Qin, Q.B., Chen, B., Ma, M., Tang, C.C., Liu, S.J., 2020a. The establishment of the fertile fish lineages derived from distant hybridization by overcoming the reproductive barriers. Reproduction 159, R237–R249. https://doi.org/10.1530/Rep-19-0576.
Liu, Y., Zhu, Z.Y., Ho, I.H.T., Shi, Y.J., Li, J.Z., Wang, X., Chan, M.T.V., Cheng, C.H.K., 2020b. Genetic deletion of *miR-430* disrupts maternal-zygotic transition and embryonic body plan. Front. Genet. 11, 853. https://doi.org/10.3389/fgene.2020.00853.
Lv, X., Wang, W., Han, Z., Liu, S., Yang, W., Li, M., Wang, L., Song, L., 2019. The dicer from oyster *Crassostrea gigas* functions as an intracellular recognition molecule and effector in anti-viral immunity. Fish Shellfish Immunol. 95, 584–594. https://doi.org/10.1016/j.fsi.2019.10.067.
McCreight, J.C., Schneider, S.E., Wilburn, D.B., Swanson, W.J., 2017. Evolution of microRNA in primates. PloS One 12. https://doi.org/10.1371/journal.pone.0176596.
Mei, J., Yue, H.M., Li, Z., Chen, B., Zhong, J.X., Dan, C., Zhou, L., Gui, J.F., 2014. *C1q-like* factor, a target of *miR-430*, regulates primordial germ cell development in early embryos of *Carassius auratus*. Int. J. Biol. Sci. 10, 15–24. https://doi.org/10.7150/ijbs.7490.
Moran, B.M., Payne, C., Langdon, Q., Powell, D.L., Brandvain, Y., Schumer, M., 2021. The genomic consequences of hybridization. Elife 10, e69016. https://doi.org/10.7554/eLife.69016.
Örkenby, L., Skog, S., Ekman, H., Gozzo, A., Kugelberg, U., Ramesh, R., Magadi, S., Zambanini, G., Nordin, A., Cantú, C., Nätt, D., Öst, A., 2023. Stress-sensitive dynamics of miRNAs and Elba1 in *Drosophila* embryogenesis. Mol. Syst. Biol. 19, e11148. https://doi.org/10.15252/msb.202211148.
Pala, I., Coelho, M.M., Schartl, M., 2008. Dosage compensation by gene-copy silencing in a triploid hybrid fish. Curr. Biol. 18, 1344–1348. https://doi.org/10.1016/j.cub.2008.07.096.
Pfaffl, M.W., Tichopad, A., Prgomet, C., Neuvians, T.P., 2004. Determination of stable housekeeping genes, differentially regulated target genes and sample integrity: BestKeeper–Excel-based tool using pair-wise correlations. Biotechnol. Lett. 26, 509–515. https://doi.org/10.1023/b:bile.0000019559.84305.47.
Ren, L., Tang, C.C., Li, W.H., Cui, J.L., Tan, X.J., Xiong, Y.F., Chen, J., Wang, J., Xiao, J., Zhou, Y., Wang, J., Tao, M., Zhang, C., Liu, S.J., 2017. Determination of dosage compensation and comparison of gene expression in a triploid hybrid fish. BMC Genomics 18, 38. https://doi.org/10.1186/s12864-016-3424-5.
Ren, L., Li, W.H., Qin, Q.B., Dai, H., Han, F.M., Xiao, J., Gao, X., Cui, J.L., Wu, C., Yan, X.J., Wang, G.L., Liu, G.M., Liu, J., Li, J.M., Wan, Z., Yang, C.H., Zhang, C., Tao, M., Wang, J., Luo, K.K., Wang, S., Hu, F.Z., Zhao, R.R., Li, X.M., Liu, M., Zheng, H.K., Zhou, R., Shu, Y.Q., Wang, Y.D., Liu, Q.F., Tang, C.C., Duan, W., Liu, S.J., 2019. The subgenomes show asymmetric expression of alleles in hybrid lineages of *Megalobramaamblycephala* × *Culter alburnus*. Genome Res. 29, 1805–1815. https://doi.org/10.1101/gr.249805.119.
Romero, I.G., Ruvinsky, I., Gilad, Y., 2012. Comparative studies of gene expression and the evolution of gene regulation. Nat. Rev. Genet. 13, 505–516. https://doi.org/10.1038/nrg3229.
Rosa, A., Brivanlou, A.H., 2017. Role of microRNAs in zygotic genome activation: modulation of mRNA during embryogenesis. Meth. Mol. Biol. (Clifton, N.J.). 1605, 31–43. https://doi.org/10.1007/978-1-4939-6988-3_3.
Song, C., Liu, S.J., Xiao, J., He, W.G., Zhou, Y., Qin, Q., Zhang, C., Liu, Y., 2012. Polyploid organisms. Sci China. Life Sci. 55, 301–311. https://doi.org/10.1007/s11427-012-4310-2.
Sun, Z.H., Wang, Y., Lu, W.J., Li, Z., Liu, X.C., Li, S.S., Zhou, L., Gui, J.F., 2017. Divergent expression patterns and function implications of four *nanos* genes in a hermaphroditic fish, *Epinephelus coioides*. Int J Mol Sci. 18. https://doi.org/10.3390/ijms18040685.
Takacs, C.M., Giraldez, A.J., 2016. *miR-430* regulates oriented cell division during neural tube development in zebrafish. Dev. Biol. 409, 442–450. https://doi.org/10.1016/j.ydbio.2015.11.016.
Tani, S., Kusakabe, R., Naruse, K., Sakamoto, H., Inoue, K., 2010. Genomic organization and embryonic expression of *miR-430* in medaka (*Oryzias latipes*): insights into the post-transcriptional gene regulation in early development. Gene 449, 41–49. https://doi.org/10.1016/j.gene.2009.09.005.
Tao, W., Sun, L., Chen, J., Shi, H., Wang, D., 2016. Genomic identification, rapid evolution, and expression of Argonaute genes in the tilapia, *Oreochromis niloticus*. Dev Genes Evol. 226, 339–348. https://doi.org/10.1007/s00427-016-0554-3.
Thisse, C., Thisse, B., 2008. High-resolution in situ hybridization to whole-mount zebrafish embryos. Nat. Protoc. 3, 59–69. https://doi.org/10.1038/nprot.2007.514.
Vastenhouw, N.L., Cao, W.X., Lipshitz, H.D., 2019. The maternal-to-zygotic transition revisited. Development 146. https://doi.org/10.1242/dev.161471.
Veil, M., Schaechtle, M.A., Gao, M., Kirner, V., Buryanova, L., Grethen, R., Onichtchouk, D., 2018. Maternal Nanog is required for zebrafish embryo architecture and for cell viability during gastrulation. Development 145. https://doi.org/10.1242/dev.155366.
Walser, C.B., Lipshitz, H.D., 2011. Transcript clearance during the maternal-to-zygotic transition. Curr. Opin. Genet. Dev. 21, 431–443. https://doi.org/10.1016/j.gde.2011.03.003.
Wang, J., Ye, L.H., Liu, Q.Z., Peng, L.Y., Liu, W., Yi, X.G., Wang, Y.D., Xiao, J., Xu, K., Hu, F.Z., Ren, L., Tao, M., Zhang, C., Liu, Y., Hong, Y.H., Liu, S.J., 2015. Rapid genomic DNA changes in allotetraploid fish hybrids. Heredity 114, 601–609. https://doi.org/10.1038/hdy.2015.3.
Wang, S., Tang, C.C., Tao, M., Qin, Q.B., Zhang, C., Luo, K.K., Zhao, R.R., Wang, J., Ren, L., Xiao, J., Hu, F.Z., Zhou, R., Duan, W., Liu, S.J., 2019. Establishment and application of distant hybridization technology in fish. Sci. China Life Sci. 62, 22–45. https://doi.org/10.1007/s11427-018-9408-x.
Wang, J., Zhang, Y.R., Wang, W., Wang, C., Wu, J.H., Wang, Y., Peng, Z.H., Liu, T., Wang, S.W., Liu, C.X., Luo, K.K., Jiang, Y.J., Deng, Y., Liu, S.J., 2025. Spatiotemporal expression patterns of maternal-zygotic gene *pou5f3* in hybrid fish embryos. Aquaculture 598, 741954. https://doi.org/10.1016/j.aquaculture.2024.741954.
Watanabe, T., Takeda, A., Mise, K., Okuno, T., Suzuki, T., Minami, N., Imai, H., 2005. Stage-specific expression of microRNAs during *Xenopus* development. FEBS Lett. 579, 318–324. https://doi.org/10.1016/j.febslet.2004.11.067.
Yu, M., Wang, F., Gang, H., Liu, C., 2024. Research progress of nanog gene in fish. Molecular genetics and genomics : MGG. 299, 88. https://doi.org/10.1007/s00438-024-02182-x.
Zhang, Z.H., Chen, J., Li, L., Tao, M., Zhang, C., Qin, Q.B., Xiao, J., Liu, Y., Liu, S.J., 2014. Research advances in animal distant hybridization. Sci. China Life Sci. 57, 889–902. https://doi.org/10.1007/s11427-014-4707-1.
Zhang, C., Wang, M., Li, Y., Zhang, Y., 2022. Profiling and functional characterization of maternal mRNA translation during mouse maternal-to-zygotic transition. Sci. Adv. 8, eabj3967. https://doi.org/10.1126/sciadv.abj3967.
Zhao, C., Zhu, W.X., Yin, S.W., Cao, Q.Q., Zhang, H.Y., Wen, X., Zhang, G.S., Xie, W.L., Chen, S.Q., 2018. Molecular characterization and expression of *Piwil1* and *Piwil2* during gonadal development and treatment with HCG and LHRH-A_2 in *Odontobutis potamophila*. Gene 647, 181–191. https://doi.org/10.1016/j.gene.2018.01.038.
Zhou, Y.W., Wang, X.K., 2014. Explore the relationship between online shopping and shopping trips: an analysis with the 2009 NHTS data. Transport Res a-Pol. 70, 1–9. https://doi.org/10.1016/j.tra.2014.09.014.
Zhou, Y., Wang, F.H., Liu, S.J., Zhong, H., Liu, Z., Tao, M., Zhang, C., Liu, Y., 2012. Human chorionic gonadotropin suppresses expression of Piwis in common carp (*Cyprinus carpio*) ovaries. Gen Comp Endocr. 176, 126–131. https://doi.org/10.1016/j.ygcen.2011.11.044.
Zhu, Z., Liu, Y., Xu, W., Liu, T., Xie, Y., Sham, K.W.Y., Sha, O., Cheng, C.H.K., 2020. Functional characterization and expression analyses show differential roles of maternal and zygotic *Dgcr8* in early embryonic development. Front. Genet. 11, 299. https://doi.org/10.3389/fgene.2020.00299.